PHYSICAL REVIEW B VOLUME 35, NUMBER 8 15 MARCH 1987-I

# Raman scattering study of coupled hole-plasmon—LO-phonon modes in $p$-type GaAs and $p$-type $Al_xGa_{1-x}As$

Tonao Yuasa* and Makoto Ishii†
*Optoelectronics Joint Research Laboratory, 1333 Kamikodanaka, Nakahara-ku, Kawasaki 211, Japan*
(Received 3 September 1986)

The hole-plasmon—LO-phonon coupling has been studied with the use of Raman scattering from Be-doped $p$-type GaAs and $p$-type $Al_xGa_{1-x}As$ layers grown by molecular-beam epitaxy. The Raman spectra from heavily doped (100) $p$-type GaAs layers show a shoulder and a broad peak on the higher- and lower-frequency sides of the LO-phonon peaks, respectively. The structures on both sides of the LO-phonon peaks are assigned to the coupled hole-plasmon—LO-phonon modes by their frequencies and dampings which are dependent on the hole concentration and by comparison with the spectra from (110) cleaved surfaces. In the Raman spectra from (100) $p$-type $Al_xGa_{1-x}As$ layers with high hole concentrations, three modes in addition to two LO-phonon branches are observed; they are identified as branches of the coupled modes by comparison with the Raman spectra of $p$-type GaAs layers, with reference to experimental results for $n$-type $Al_xGa_{1-x}As$ layers. The coupling between single-particle hole excitations and TO phonons is also discussed for the spectra from the (110) surfaces of $p$-type GaAs with different hole concentrations.

## I. INTRODUCTION

Electronic excitations in semiconductors interact with optical phonons. The single-particle and collective electronic excitations (plasmons) coupled with optical phonons have been extensively studied in ZnS-type semiconductors with the use of Raman spectroscopy. In degenerate binary semiconductors, two long-wavelength ($q \sim 0$) coupled plasmon—longitudinal-optical (LO)-phonon collective modes participate in the first-order Raman scattering. The coupled modes have been investigated particularly in $n$-type GaAs, and the behavior of the modes denoted by $L_+$ and $L_-$ is well understood.[1-4] The frequencies and intensities of the Raman modes change as a function of electron concentration. When electron concentration increases, the $L_+$ mode weakens, and shifts from the LO-phonon frequency to the higher-frequency side, while the $L_-$ mode strengthens, and approaches the transverse-optical (TO)-phonon frequency from the lower-frequency side. The electron-plasmon—LO-phonon coupling has also been measured for mixed crystals by Raman scattering. The number of coupled-mode branches increases with increasing number of LO-phonon branches in some mixed crystals. Three Raman lines due to the coupling have recently been observed in $n$-type $Al_xGa_{1-x}As$ with two LO-phonon modes.[5,6]

The interaction between single-particle hole excitations and TO phonons has been studied in $p$-type semiconductors. The shifts and broadenings of the TO phonons by the interaction are observed in the Raman spectra of $p$-type Si,[7] $p$-type Ge,[8] and $p$-type GaAs.[9] Little is known about the free-hole—LO-phonon coupling, compared to the single-particle-hole—TO-phonon and the free-electron—LO-phonon couplings. The reason is mainly due to difficulties in obtaining degenerate $p$-type samples. The effective masses of free holes in many semiconductors are much larger than those of electrons. The large effective masses produce a large density of states in the valence bands, which requires heavy doping to make the free carriers degenerate. Olego and Cardona[9] have investigated Raman spectra in Zn-doped $p$-type bulk (100) GaAs, and observed two free-hole-related lines near the LO- and the forbidden TO-phonon frequencies in the heavily doped samples. Processes in which the wave vector is not conserved have been observed in resonant Raman and luminescence studies of $p$-type GaAs.[10,11] The wave-vector nonconservation induces the large-wave-vector $L_-$ mode which lies at a slightly lower-frequency side of the LO phonons, and allows the appearance of the forbidden optical phonons in the Raman spectra.[3,10] For this reason, they have assigned the two lines to the $L_-$ mode with large wave-vectors and the forbidden TO phonons. On the other hand, they claim that no evidence was found for the long-wavelength coupled modes in Ref. 9. However, the crystalline quality limits the observability of the coupled modes. For example, a spatial variation of the dopant distribution causes inhomogeneous broadening of the coupled modes, and precipitation of the impurities spreads the coupled-mode lines with an increased scattering rate.[1,4] These damping mechanisms weaken the coupled-mode signals, and therefore make it difficult to observe them.

In this paper, we measure the coupled hole-plasmon—LO-phonon modes in Be-doped $p$-type GaAs and $Al_xGa_{1-x}As$ layers grown by molecular-beam epitaxy (MBE) with the use of Raman scattering. Beryllium has been extensively used as an almost ideal $p$-type dopant in MBE growth of GaAs and $Al_xGa_{1-x}As$ for fabricating electrical and optical devices.[12,13] The doping levels up to the mid-$10^{19}$-$cm^{-3}$ range have been achieved in both GaAs and $Al_xGa_{1-x}As$ while maintaining surface morphologies and hole mobilities comparable to those obtained in liquid-phase epitaxy. Low-threshold current densities of GaAs/$Al_xGa_{1-x}As$ double-heterostructure

 

lasers with Be-doped $p$-type $Al_xGa_{1-x}As$ cladding layers demonstrate that excellent optical properties can be obtained with this acceptor dopant.[14] The high-crystalline quality in heavily Be-doped samples should facilitate the observation of coupled free-hole-plasmon—LO-phonon modes in the Raman spectra. The organization of the paper is as follows. The details of the experimental procedure are described in Sec. II. Following this, Sec. III presents the experimental results on $p$-type GaAs and $p$-type $Al_xGa_{1-x}As$. In Sec. IV, the coupling between single-particle hole excitations and TO phonons as well as the identification of the coupled modes are discussed in the light of previous experiments.

## II. EXPERIMENTAL

The Be-doped $p$-type GaAs and $p$-type $Al_xGa_{1-x}As$ layers were grown on Cr-doped (100) semi-insulating GaAs substrates by MBE. The growth was carried out using a three-chamber Varian MBE GEN II system, which provides excellent uniformity in doping profiles in addition to the uniformity in layer thickness and the alloy composition over a large area, because of precise control of beam fluxes and rotation of a substrate holder. Substrate preparation and growth conditions are similar to those described earlier.[6] Elemental Al, Ga, As, and Be were used as source materials.

For all samples, a 0.5-$\mu$m-thick unintentionally doped GaAs buffer layer was first grown on the semi-insulating GaAs substrate to obtain a good crystalline quality for the succeeding $\sim$3-$\mu$m-thick $p$-type GaAs and $\sim$2-$\mu$m-thick $p$-type $Al_xGa_{1-x}As$ layers. Differently doped $p$-type GaAs layers were grown on the different substrates. On the other hand, differently doped $Al_xGa_{1-x}As$ layers with a fixed alloy composition were successively grown on a same GaAs substrate by only changing the temperature of the Be source to keep the alloy composition of each layer at constant. The hole concentrations of $p$-type GaAs layers were obtained by Hall measurements. The hole concentrations of $p$-type $Al_xGa_{1-x}As$ layers were determined with the use of the Hall data of other $p$-type $Al_xGa_{1-x}As$ layers with the same alloy composition grown on semi-insulating GaAs substrates at the same temperatures of the Be source.

Crystalline quality of Be-doped grown layers was measured by photoluminescent (PL) emission. The PL intensity increased almost linearly with increasing hole concentration to the high hole concentrations above $1\times10^{19}$ $cm^{-3}$. The PL results demonstrate high quality of the heavily Be-doped layers.

The Raman scattering from the samples was studied at room temperature with the main use of the 514.5-nm line of a Spectra Physics model 164 Ar-ion laser operated at 200—500 mW, in the standard backscattering geometry. The 488.0-nm line of the laser was also used to study the wave-vector dependence of some spectra. The laser beam formed an illuminated area of $\sim$200 $\mu$m in diameter on the sample surfaces. The scattered light was collected in a direction normal to the surface and focused onto the entrance slit of a Jobin-Ybon RAMANOR U-1000 double monochromator equipped with 1800-lines/mm holographic gratings. A cooled Hamamatsu R-649 photomultiplier tube was used for the detector along with standard photon-counting equipment. The counts were stored on a multichannel analyzer with integration times per channel ranging from 0.4 to 1 sec. A low-pressure Hg lamp was used for wavelength-calibration purposes. The spectra was recorded with a spectral resolution between 1 and 4 $cm^{-1}$ on an $X$-$Y$ plotter.

## III. EXPERIMENTAL RESULTS

### A. $p$-type GaAs

#### 1. Hole-concentration dependence

The Stokes Raman spectra of $p$-type GaAs layers were measured for a wide range of hole concentration starting at $1\times10^{16}$ $cm^{-3}$ and up to $2\times10^{19}$ $cm^{-3}$ for an excitation wavelength of 514.5 nm. The results in the frequency range between 350 and 240 $cm^{-1}$ are shown for some typical spectra of the samples with different hole concentrations in Fig. 1. The measurements were performed under the same conditions. Accordingly, the intensities of the peaks in Fig. 1 can be compared with each other. Only LO phonons, which are allowed for scattering from the (100) surfaces in backscattering geometry, are observed at 292 $cm^{-1}$ for lightly doped $p$-type GaAs layer with a hole concentration ($p$) of $1\times10^{16}$ $cm^{-3}$. The LO-phonon mode is observed for all hole concentrations. However, its intensity decreases with increasing hole concentration. For the sample with $p=3\times10^{18}$ $cm^{-3}$, a shoulder denoted $A$ appears on the high-frequency side of the LO-phonon mode, and a weak shoulder denoted $B$ also appears on the low-frequency side of the LO-phonon mode.

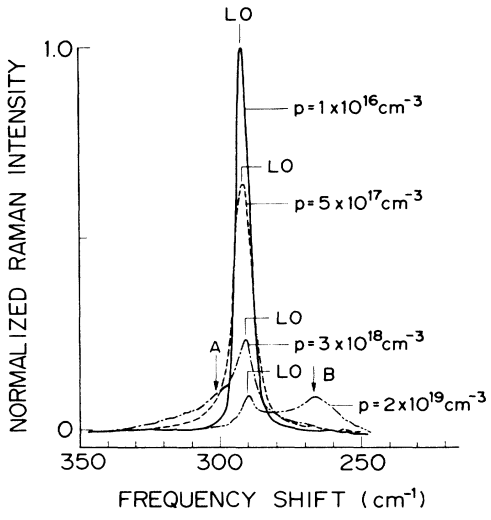


FIG. 1. Raman spectra from (100) $p$-type GaAs layers with hole concentrations ranging from $1\times10^{16}$ to $2\times10^{19}$ $cm^{-3}$. These spectra were obtained with the 514.5-nm line of an Ar-ion laser. The line labeled LO is the longitudinal-optical (LO)-phonon mode. The arrows labeled $A$ and $B$ represent the coupled hole-plasmon—LO-phonon modes.

When the hole concentration increases up to $2\times10^{19}$ $cm^{-3}$, the shoulder $A$ disappears while the shoulder $B$ grows into a broadband peaking around 266 $cm^{-1}$. The peak frequency of the band $B$ is near the TO-phonon one (268 $cm^{-1}$).

The linewidth of the LO-phonon mode also changes with increasing hole concentration. To compare correctly the widths and profiles of the Raman lines, the spectra in Fig. 1 are rewritten as shown in Fig. 2. In Fig. 2, the peak heights of the LO-phonon mode are normalized to unity. The LO-phonon mode broadens initially with a slight increase of peak frequency for hole concentrations up to $3\times10^{18}$ $cm^{-3}$, and then narrows with a decrease of the peak frequency for $2\times10^{19}$ $cm^{-3}$. For the sample with $p=1\times10^{16}$ $cm^{-3}$, the phonon profile shows symmetry of Lorentzian type which has been investigated on phonon profiles of binary semiconductors such as GaAs,[15] and GaP.[16] However, the profile becomes asymmetric with a high-frequency tail for the sample with $p=5\times10^{17}$ $cm^{-3}$. The change in linewidth at the high-frequency side is noticeable, while that at the low-frequency side is very slight. Asymmetry of the phonon-line profile for $p=3\times10^{18}$ $cm^{-3}$ is enhanced by the two shoulders with different intensities. Shoulder $A$ at the high-frequency side of the LO-phonon mode is much stronger as compared with shoulder $B$ on the low-frequency side, but shoulder $A$ vanishes for the sample with $p=2\times10^{19}$ $cm^{-3}$, resulting in the narrow LO-phonon line. In addition, no additional structure due to the shift of shoulder $A$ was observed in the higher-frequency range. The intensity of the band $B$ is so high that it is comparable to that of the LO phonons, and the band markedly spreads compared to the LO-phonon line. It is noted that the peak frequency (266 $cm^{-1}$) of the band $B$ is slightly below the TO-phonon frequency (268 $cm^{-1}$).

Figure 3 shows the linewidth and the peak frequency of the LO-phonon mode as a function of the hole concentration. The peak frequencies were determined to an accuracy of 0.3–0.5 $cm^{-1}$. The linewidth, which is defined as the full width at half maximum, increases from 5 to 15 $cm^{-1}$ for hole concentrations ranging from $1\times10^{16}$ to

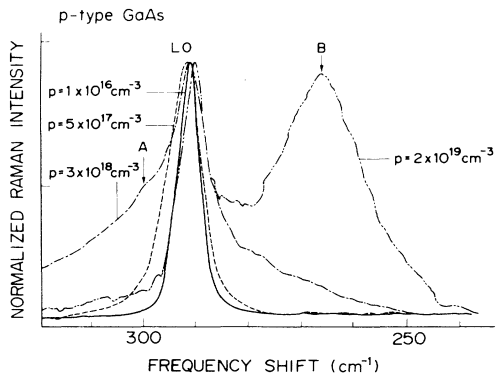


FIG. 2. Spectra are rewritten from Fig. 1. We note that Raman intensity is normalized by each peak intensity of the LO-phonon mode.

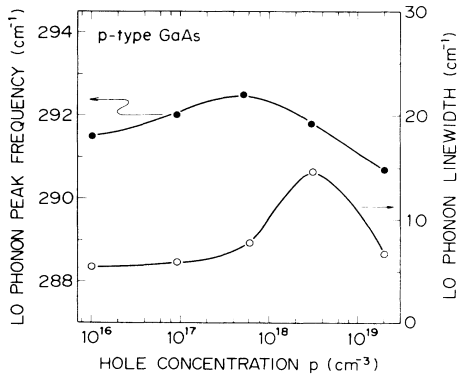


FIG. 3. Peak frequency and linewidth of the LO-phonon mode in $p$-type GaAs as a function of hole concentration. After the initial increases with increasing hole concentration, both the peak frequency and the halfwidth decrease for very high hole concentrations. The large halfwidth at $p=3\times10^{18}$ $cm^{-3}$ contains partly the shoulder of the high-frequency coupled mode.

$3\times10^{18}$ $cm^{-3}$. The width, however, decreases to 6 $cm^{-1}$ for $p=2\times10^{19}$ $cm^{-3}$. The peak frequency increases slightly by about 1 $cm^{-1}$ for a hole concentration ranging from $1\times10^{16}$ to $5\times10^{17}$ $cm^{-3}$, and then decreases for higher hole concentrations. The peak frequency for $p=2\times10^{19}$ $cm^{-3}$ is lower than that for $p=1\times10^{16}$ $cm^{-3}$ by about 1 $cm^{-1}$.

Referring to Raman studies for the coupled electron-plasmon–LO-phonon modes in $n$-type GaAs,[1–4] we can interpret the behavior of the LO-phonon mode, $A$ and $B$ modes in Figs. 1–3 as due to the interaction between the free holes and the LO phonons. According to Raman experiments on $n$-type GaAs, we observe both the coupled electron-plasmon–LO phonons from the bulk and the unscreened LO phonons from the surface depletion layer in the spectra of $n$-type GaAs. As the carrier concentration increases, the high-frequency branch of the coupled modes shifts to the higher-frequency side with decreasing the intensity, and the signal of the unscreened LO phonons weakens because of the decrease in the depletion-layer depth. At the electron concentration below $\sim5\times10^{17}$ $cm^{-3}$, the frequency shift of the coupled mode is very small. Therefore, the unscreened and the coupled LO phonons are observed as one line in the Raman spectra. This superimposition effect can explain the initial slight peak shift and high-frequency tail of the LO-phonon line for $p$-type GaAs layers with hole concentrations between $1\times10^{16}$ and $5\times10^{17}$ $cm^{-3}$ in Figs. 1–3 as follows. The penetration depth is $\sim1000$ Å at the wavelength of 514.5 nm. On the other hand, when the hole concentration increases from $1\times10^{16}$ to $5\times10^{17}$ $cm^{-3}$, the depletion-layer width decreases from $\sim3000$ to $\sim400$ Å, and the high-frequency branch of the coupled modes damps with a slight shift to the higher-frequency side, resulting in weakening, spreading, and shifting of the LO-phonon mode composed of both the unscreened component from the depletion layer and the coupled component from the bulk. When the hole concentration increases up to $3\times10^{18}$ $cm^{-3}$, the coupled LO phonons shift

further to the higher-frequency side, separating from the unscreened LO phonons. The two LO-phonon modes are no longer observed as one line in the spectra. Consequently, the peak of the LO-phonon mode returns to the position of the unscreened LO-phonon mode. The large linewidth for $p=3\times10^{18}$ cm$^{-3}$ is merely due to addition of the broad width of the mode $A$. The large effective mass of free holes introduces the large damping constant of the coupled LO phonons through the smaller mobilities. In addition, the damping constant increases with increasing hole concentration, accompanying the larger plasmon component.[1,17] Such a very large damping constant should make it difficult to observe the coupled LO phonons for the samples with high hole concentrations because of markedly broadening the coupled modes. Actually, the indication of the high-frequency branch of the coupled modes was not clearly found in the measured spectrum for the sample with $p=2\times10^{19}$ cm$^{-3}$. The detailed evaluation of the damping constant will be described later. The $L_-$ mode with a sharp profile locates near the TO phonons for heavily doped $n$-type GaAs.[1-4] This fact leads to the assignment of mode $B$ at 266 cm$^{-1}$ for $p=3\times10^{18}$ and $1\times10^{19}$ cm$^{-3}$ to the low-frequency branch of the coupled modes. The large broadening of mode $B$ is due to the low hole mobility. A slight decrease in the unscreened LO-phonon frequency for $p=1\times10^{19}$ cm$^{-3}$ is possibly associated with softening of the crystal, that is, reduction in the elastic constants by a number of carriers.[18]

### 2. *Wave-vector dependence*

The relative intensities of the unscreened LO phonons and the coupled ones depend on the excitation wavelength because the penetration depth is a function of the excitation wavelength. Figure 4 shows the Raman spectra of the samples with $p=3\times10^{18}$ and $2\times10^{19}$ cm$^{-3}$, which have been obtained with the 488.0- and 514.5-nm lines of an Ar-ion laser. As can be seen, the $A$ and $B$ coupled-mode signals relative to the LO phonons for the excitation wavelength of 488.0 nm are smaller than those for the excitation of the 514.5-nm line. The depth of the surface depletion is less than 200 Å for the hole concentration above $1\times10^{18}$ cm$^{-3}$, while the penetration depth into GaAs varies approximately from 1000 Å for 514.5 nm to 900 Å for 488.0 nm. Such a decrease in the penetration depth explains the decreases in the intensity ratios of the coupled modes in the bulk region to the LO phonons in the surface depletion region in Fig. 4. The frequencies of the coupled modes are almost unchanged for the different excitation wavelengths, as seen in Fig. 4. The results indicate that the wave-vector dependence of the coupled hole-plasmon—LO-phonon modes is small. On the other hand, the large wave-vector dependence of the coupled electron-plasmon—LO-phonon modes is observed in $n$-type GaAs.[2-4] For a given electron concentration, the high-frequency coupled mode $L_+$ shifts to higher frequencies with increasing wave vector, that is, decreasing excitation wavelength. The low-frequency coupled mode $L_-$ also shifts to higher frequencies and approaches the LO-phonon frequency. The large-frequency dispersion effect

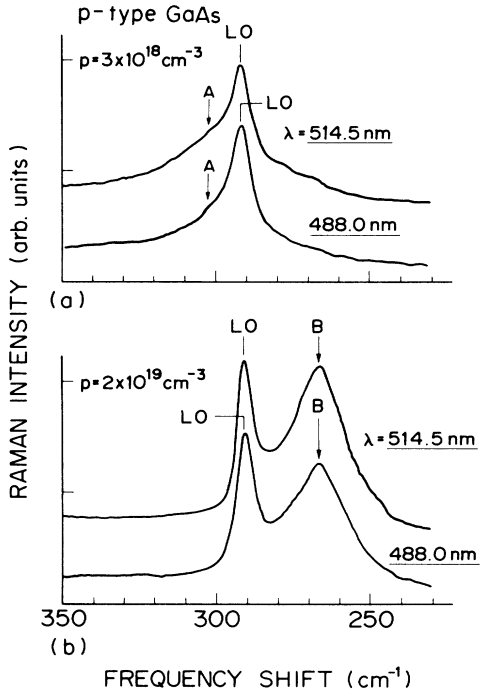


FIG. 4. Raman spectra from the (100) surfaces of heavily doped $p$-type GaAs layers with (a) $p=3\times10^{18}$ and (b) $2\times10^{19}$ cm$^{-3}$ at two different laser-excitation wavelengths ($\lambda$). The spectra for $\lambda=514.5$ nm are the same as those in Fig. 1. The intensity ratios of the coupled modes $A$ and $B$ to the LO-phonon mode decrease with decreasing excitation wavelength.

in the electron-plasmon-phonon system arises from the large-frequency dispersion of the electron plasma. The wave-vector-dependent plasma frequency can be approximately written as[4,6]

$$\omega_p^2(q)\sim\omega_p^2+\tfrac{3}{5}(qv_0)^2\ , \tag{1}$$

with

$$\omega_p^2=4\pi ne^2/\epsilon_\infty m^* \tag{2}$$

and

$$v_0=\hbar(3\pi^2n)^{1/3}/m^*\ , \tag{3}$$

where $\omega_p$ is the plasma frequency when the hole interactions are screened, $\epsilon_\infty$ is the high-frequency dielectric constant, $v_0$ is the Fermi velocity, $n$ is the carrier concentration, $q$ is the wave vector, and $m^*$ is the effective mass of the carriers. Equation (1) indicates that the wave-vector dependence of the plasma frequency depends on $v_0$. The Fermi velocity of the free holes is small because of the large effective mass, as indicated in Eq. (3). Therefore, the wave-vector dependence of the hole-plasmon gas is so weak that the frequency shifts of the coupled modes cannot be clearly observed.

### 3. *Crystal orientation dependence*

Raman scattering from the forbidden optical phonons has been reported in heavily doped GaAs, and the break-

down of the selection rule for TO scattering has been explained by the wave-vector nonconservation attributed to the elastic scattering by the ionized impurities.[10] In addition, frequency shifts and broadening for allowed optical phonon lines, have been measured in the heavily doped materials. For (110)-oriented $p$-type GaAs, the TO Raman line shifts to the lower-frequency side and becomes broadened compared with the undoped material when the hole concentration exceeds $10^{19}$ cm$^{-3}$.[8] The mode $B$ shows broadening with a peak very close to the TO-phonon frequency, as shown in Fig. 1. The results mentioned above indicate the possibility of the identification of the mode $B$ as the forbidden TO phonon. However, the spectrum from (100) surfaces does not distinguish whether the mode $B$ originates from forbidden TO-phonon scattering or plasmon—LO-phonon coupling, because the two mechanisms are both possible in the configuration. In order to isolate the behavior of the TO phonons in our heavily doped samples, we have performed Raman scattering measurements from (110) cleaved surface in the backscattering geometry. For this orientation of the sample surface, Raman scattering from the LO phonons and the coupled plasmon—LO-phonon modes is forbidden, while TO-phonon scattering is allowed. For the measurements, a 514.5-nm Ar-ion laser beam was focused on the cleaved surfaces with a spot size of $\sim 1$ $\mu$m.

Figure 5 shows spectra from the (100) and (110) surfaces for a layer with $p = 2\times 10^{19}$ cm$^{-3}$. The spectrum from the (100) surface is the same as that shown in Fig. 1. The spectrum from the (110) cleaved surface reveals only the TO-phonon peak at 266 cm$^{-1}$ according to the selection rule. There is no indication of the LO phonons. In addition, no unusual broadening of the TO phonons is seen. The linewidth of the sharp TO-phonon mode from the (110) surface is 5 cm$^{-1}$, while the broad $B$ mode from the (100) surface shows a width of 20 cm$^{-1}$. The above

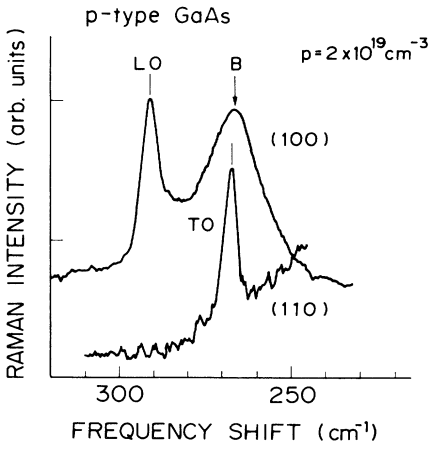


FIG. 5. Raman spectra from both the (100) and (110) surfaces of $p$-type GaAs layer with $p = 2\times 10^{19}$ cm$^{-3}$. The (110) surface was obtained by cleaving the sample. A focused 514.5-nm Ar-ion laser beam with a spot size of $\sim 1$ $\mu$m was used to measure Raman scattering from the (110) surface.

results lead to a conclusion that momentum of the incident phonons is conserved for Raman scattering, and the selection rule is maintained in the sample, and therefore mode $B$ should not be identified with the forbidden TO phonons. Thus, our interpretation of mode $B$ identifies it with the low-frequency branch of the coupled hole-plasmon—LO-phonon modes.

As mentioned above for Figs. 1 and 2, in spite of the existence of the low-frequency branch, we were not able to detect the high-frequency branch in the spectrum from the (100) surface of the heavily doped sample. By comparing with the behavior of the coupled modes $L_+$ and $L_-$ in $n$-type GaAs, we discuss in detail the reason why the high-frequency branch is not seen in the spectrum from $p$-type GaAs with $p = 2\times 10^{19}$ cm$^{-3}$. The coupled-mode intensity decreases and the mode damping increases upon increasing the ratio of the plasmon content to the phonon content.[17] At higher carrier concentrations, the $L_+$ mode becomes plasmonlike. Consequently, the mode weakens, and the damping is essentially dominated by the plasmon damping. In heavily doped samples, impurity scattering determines the scattering rate for electrons, i.e., the plasmon damping, and the scattering rate by impurities increases with increasing donor concentration. The increased electron scattering rate causes the broadening of the plasmonlike coupled mode. The electron scattering rate $1/\tau$ can be deduced from the mobility $\mu$ as $1/\tau = e/m^*\mu$.[4] Very low hole mobility for heavily doped $p$-type GaAs implies a large scattering rate for the hole plasmon, and results in the large broadening of the coupled mode. For an example of $n$-type GaAs, the observed halfwidth was $\sim 80$ cm$^{-1}$ for the $L_+$ mode of the sample with $n = 2\times 10^{18}$ cm$^{-3}$ and $\mu = 2000$ cm$^2$/V sec. From this result on $n$-type GaAs and the above relation for the electron scattering rate, the halfwidth of $\sim 302$ cm$^{-1}$ is roughly estimated from the coupled mode for the sample with $p = 2\times 10^{19}$ cm$^{-3}$ and $\mu = 75$ cm$^2$/V sec, as the halfwidth is proportional to $1/\tau$, using the heavy-hole effective mass of $0.48 m_0$ and the electron effective mass of $0.068 m_0$. Such significant broadening and weakening obstruct the detection of the $L_+$ mode. Inhomogeneous broadening, which comes from a spatial variation of the acceptor distribution, would further spread the width of the high-frequency branch. As shown in Fig. 5, the low-frequency branch is clearly observed because of its large phonon content. However, the linewidth is much wider than that of the low-frequency branch from heavily doped $n$-type GaAs. This is also possibly owing to the large hole-plasmon damping.

### B. $p$-type $Al_xGa_{1-x}As$

The $Al_xGa_{1-x}As$ ternary alloy has two sets of optical phonons, denoted GaAs-like and AlAs-like, over the entire composition, and the two longitudinal branches of the phonons couple strongly with the electron plasmons in the materials with direct band gap, as clearly seen in the Raman spectra of $n$-type $Al_xGa_{1-x}As$ layers.[5,6] The coupled modes consist of three branches at high frequency, low frequency, and intermediate frequency which depend on both the carrier concentration and alloy composition.

The high-frequency branch shifts from the AlAs-like LO-phonon frequency to the higher-frequency side with increasing carrier concentration. The low-frequency branch approaches the GaAs-like TO phonon from the lower-frequency side, and the intermediate-frequency branch shifts from the GaAs-like LO-phonon frequency to the AlAs-like TO-phonon frequency. In the limit of high carrier concentration, the low and intermediate branches are located at the GaAs- and AlAs-like TO-phonon positions, respectively. Hole-plasmon—LO-phonon coupling is also expected in $p$-type $Al_xGa_{1-x}As$ from the resemblance to the electron-plasmon—LO-phonon coupling in $n$-type $Al_xGa_{1-x}As$ and the hole-plasmon—LO-phonon coupling in $p$-type GaAs. Figure 6 shows the Raman spectra from the $p$-type $Al_{0.2}Ga_{0.8}As$ layers with various hole concentrations. The alloy composition is constant for all samples, because the $Al_{0.2}Ga_{0.8}As$ layers were grown successively on a GaAs substrate. Each $Al_{0.2}Ga_{0.8}As$ layer is separated by a 0.5-$\mu$m-thick undoped GaAs marking layer. The spectra were measured under the same conditions using the 514.5-nm line of the Ar-ion laser. The Raman intensities of the spectra can be compared with each other. Only sharper GaAs- and AlAs-like LO phonons are seen in the sample with the lowest hole concentration of $p=2\times10^{16}$ cm$^{-3}$, at 282 and 371 cm$^{-1}$, respectively. The intensities of the two LO phonons decrease with increasing hole concentration, as it is observed for $p$-type GaAs in Fig. 1. Figure 7 shows the

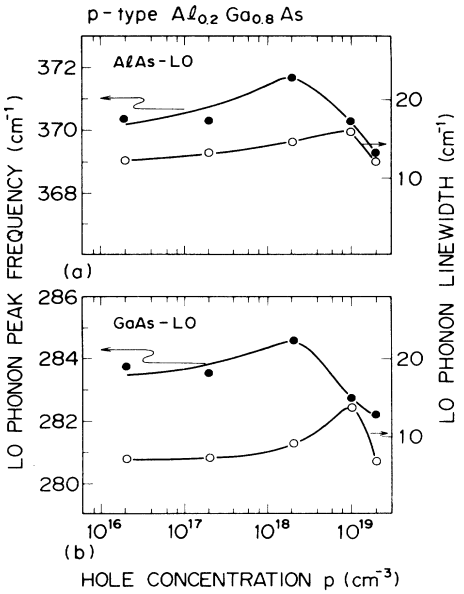


FIG. 7. Peak frequencies and linewdiths of (a) the AlAs- and (b) GaAs-like LO-phonon modes in $p$-type $Al_{0.2}Ga_{0.8}As$ as a function of hole concentration. The dependence of the peak frequencies and the linewidths on hole concentration is similar to that for $p$-type GaAs in Fig. 3.

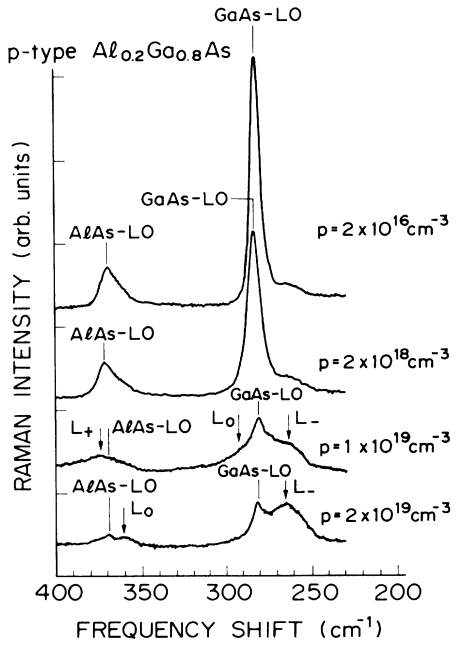


FIG. 6. Raman spectra from (100) $p$-type $Al_{0.2}Ga_{0.8}As$ layers with hole concentrations ranging from $2\times10^{16}$ to $2\times10^{19}$ cm$^{-3}$. The spectra were obtained with $\lambda=514.5$ nm. The arrows labeled $L_+$, $L_0$, and $L_-$ are the coupled hole-plasmon—LO-phonon modes. Sharp peaks labeled GaAs-LO and AlAs-LO are the GaAs- and AlAs-like branches of the LO phonons in $Al_xGa_{1-x}As$.

linewidths and the peak frequencies of the GaAs- and AlAs-like LO phonons as a function of the hole concentration. The hole concentration dependence of the linewidths and frequencies of the LO phonons is very similar to that for $p$-type GaAs in Fig. 3. The determination of the peak frequencies was made to an accuracy of 0.5 cm$^{-1}$ except the AlAs LO-phonon frequency for $p=1\times10^{19}$ cm$^{-3}$ (the accuracy is larger than 2 cm$^{-1}$). For the sample with $p=2\times10^{18}$ cm$^{-3}$, the LO phonons shift to the higher-frequency side by about 1 cm$^{-1}$, and their halfwidths are somewhat wider than those of the sample with $p=1\times10^{16}$ cm$^{-3}$. When $p$ increases to $1\times10^{19}$ cm$^{-3}$, the LO phonons return to the lower-frequency positions, and for $p=2\times10^{19}$ cm$^{-3}$, they still shift to the lower-frequency sides with the decrease in the linewidths. The frequency shifts can be explained by considering hole-plasmon—LO-phonon coupling and LO phonons from the surface depletion layer, as described above for Fig. 3. In our measurements, we observe the Raman signals from both the bulk and depleted surface of the $p$-type $Al_xGa_{1-x}As$ layers, simultaneously. When the hole concentration increases, the GaAs- and AlAs-like LO phonons show apparently slight shifts to the higher-frequency sides due to the coupling to the hole plasmons, and then they return to the lower-frequency sides due to the separation of the coupled modes from the LO phonons; the two LO-phonon modes from the depleted surface are seen without the coupling component in the spectra.

Some shoulders appear on the high- and low-frequency sides of the AlAs-like LO-phonon peaks in the spectrum for $p=1\times10^{19}$ cm$^{-3}$ in Fig. 6. For the highest hole con-

centration of $p=2\times10^{19}$ cm$^{-3}$, the broad structures are clearly seen on the low-frequency sides of the two LO-phonon peaks. In order to make clear the hole concentration dependence of the additional structures, the spectra for $p=1\times10^{16}$, $1\times10^{19}$, and $2\times10^{19}$ cm$^{-3}$ in Fig. 6 were rewritten, as shown in Fig. 8. The Raman intensities are normalized by the intensity of the GaAs-like LO phonons in the layer with $p=2\times10^{16}$ cm$^{-3}$. The shoulder labeled $L_-$ on the low-frequency side of the GaAs-like LO phonon grows up to the broadband at the GaAs-like TO-phonon position in the spectrum for $2\times10^{19}$ cm$^{-3}$, and the shoulder labeled $L_0$ on the high-frequency side of the LO phonon vanishes. The broad structure designated $L_+$, which overlaps at the high-frequency tail of the AlAs-like LO phonon, is not seen in the spectrum for $p=2\times10^{19}$ cm$^{-3}$, and instead the peak $L_0$ appears at the AlAs-like TO-phonon position. Thus, the hole-concentration-dependent behavior of the $L_+$, $L_-$, $L_0$ modes and the LO phonons is very similar to that of the coupled modes in $p$-type GaAs for Figs. 1 and 2. Accordingly, the $L_+$, $L_-$, and $L_0$ modes are assigned to the coupled hole-plasmon—LO-phonon modes. They correspond to the high-, low-, and intermediate-frequency branches of the coupled electron-plasmon—LO-phonons. When the hole concentration increases, the $L_+$ mode shifts from the GaAs-like LO-phonon frequency to the higher-frequency side with the increase in damping. The too large damping makes it very difficult to observe the $L_+$ mode in the spectrum for $p=2\times10^{19}$ cm$^{-3}$. The $L_-$ mode approaches the GaAs-like TO-phonon frequency with the decrease in damping. However, the low hole mobilities cause the broadening of the mode even for $p=2\times10^{19}$ cm$^{-3}$, as shown in Figs. 6 and 7. The $L_0$ mode approaches the AlAs-like TO-phonon frequency, separating from the GaAs-like LO phonon. The phonon content of the $L_0$ mode is large at both very low and very high hole concentrations, while it is small at intermediate hole concentrations.[6] Consequently, the mode is clearly observed near the AlAs-like TO-phonon frequency in the spectrum for $p=2\times10^{19}$ cm$^{-3}$. The large damping of the hole plasmon can increase rapidly the $L_0$ mode frequency with increasing hole concentration,[19] as shown in the spectra for $p=1\times10^{19}$ and $2\times10^{19}$ cm$^{-3}$.

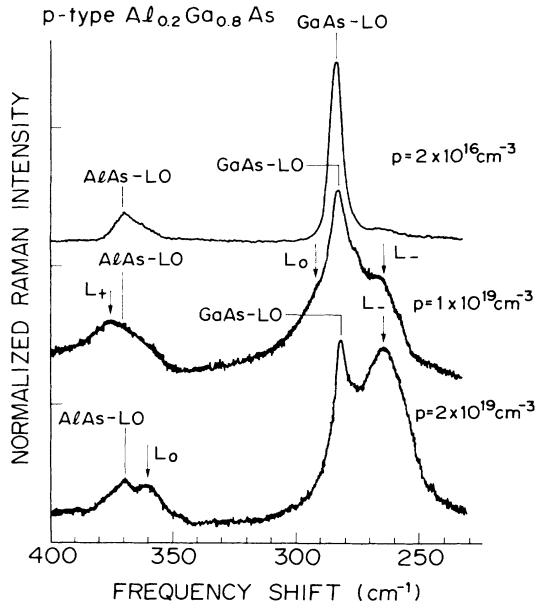


FIG. 8. Spectra for $p=2\times10^{16}$, $1\times10^{19}$, and $2\times10^{19}$ cm$^{-3}$ are rewritten from Fig. 6. Raman intensity is normalized by each peak intensity of the GaAs-like LO-phonon mode.

The behavior of the coupled modes in $p$-type $Al_xGa_{1-x}As$ with other alloy compositions is similar to that in $p$-type $Al_{0.2}Ga_{0.8}As$. However, for larger alloy compositions, the coupled modes for a given hole concentration shift to lower-frequency sides, and still broaden, because the values of both $m^*$ and $m^*\epsilon_\infty$ in Eqs. (1)—(3) become larger.

## IV. DISCUSSION

Raman scattering from heavily Zn-doped $p$-type bulk GaAs has been studied by Olego and Cardona.[9] They have observed two Raman lines whose frequencies and halfwidths depend on the hole concentration; one line is the LO-like mode which peaks at around 295 cm$^{-1}$, the other line is the TO-like mode which peaks at around 271 cm$^{-1}$, and the two lines shift to the lower-frequency side with increasing hole concentration. The LO-like and TO-like modes were interpreted as the coupled plasmon—LO-phonon mode with large wave vectors, and the forbidden TO phonons, respectively, in their study. The wave-vector nonconservation and the breakdown of the selection rules were attributed to elastic scattering of the photocreated carriers by the ionized acceptor impurities. In contrast, our Raman spectra indicate the conservation of the wave vectors and the selection rules even in the heaviest Be-doped materials, as shown in the spectrum from the (110) surface of Fig. 5. In addition, there are some differences between the experimental results of Olego and Cardona, and ours. In their Raman spectra, the intensity of the LO-like phonon mode increases for intermediate hole concentrations with a remarkable decrease for concentrations above $10^{19}$ cm$^{-3}$ in the LO-phonon allowed configuration, while the LO-phonon intensity decreases monotonously with increasing hole concentration in our experiments. The TO-like mode is seen for a hole concentration ranging from $10^{17}$ to $10^{20}$ cm$^{-3}$ in the spectra from the Zn-doped GaAs. On the other hand, there are no indications of the additional modes at around the TO-phonon frequency in our spectra for the hole concentrations below $1\times10^{18}$ cm$^{-3}$. The intensity ratio of the TO-like mode to the LO-like one increases with increasing hole concentration, and equals to unity for a hole concentration between $5\times10^{18}$ and $8\times10^{18}$ cm$^{-3}$ in their spectra. On the contrary, our results show that the ratio is less than unity even for a high concentration of $1\times10^{19}$ cm$^{-3}$. These differences are probably related to the crystal qualities. Crystal imperfection such as precipitates and defects in the heavily Zn-doped GaAs possibly breaks partly the selection rules and strengthens the TO-like mode in the spectra.

Olego and Cardona insist that they did not observe the long-wavelength coupled plasmon—LO-phonon modes and the unscreened LO phonon of the depletion layer.[9] However, a shoulder at the higher-frequency side of the LO phonon peak, which is assigned to the high-frequency branch of the coupled modes in our work, appears in their spectra for the samples with $p=2-5\times10^{18}$ cm$^{-3}$, and the TO-like mode for very large hole concentrations above $4\times10^{19}$ cm$^{-3}$ is characterized as the low-frequency branch of the coupled mode corresponding to the completely screened LO phonons by themselves. The unscreened LO phonons should be observed in the visibly excited Raman scattering experiments, because the thickness of the depletion layer is not negligible compared with the penetration depth of the incident laser light for all hole concentrations. The behavior of the LO-like and TO-like modes in the Zn-doped GaAs can be explained reasonably by considering that the LO-like mode contains the high-frequency branch of the coupled modes for a hole concentration below $\sim1\times10^{19}$ cm$^{-3}$ and the TO-like mode contains the low-frequency branch for a hole concentration above $\sim2\times10^{18}$ cm$^{-3}$, as described in Sec. III.

We have interpreted the hole-concentration dependence of the LO-phonon intensities in Figs. 1 and 6 as the change in the thickness of the surface depletion layer. However, the coupled modes should be strictly taken into account, because the coupled-mode components are included in the LO-phonon modes on the Raman spectra at the hole-concentration ranges below $\sim1\times10^{18}$ cm$^{-3}$ for $p$-type GaAs and below $\sim5\times10^{18}$ cm$^{-3}$ for $p$-type $Al_{0.2}Ga_{0.8}As$. Figure 9 shows the LO-phonon intensities of both $p$-type GaAs and $p$-type $Al_{0.2}Ga_{0.8}As$ layers as a function of hole concentration. Although the ratio of the decrease in the depletion depth to the increase in the hole concentration for $Al_{0.2}Ga_{0.8}As$ is almost the same as that for GaAs, reduction in the LO-phonon intensities of $p$-type $Al_{0.2}Ga_{0.8}As$ occurs at higher hole concentrations than that of $p$-type GaAs. This is mainly due to the difference in the degree of the separation of the coupled modes from the LO phonons at the same hole concentration. The coupled modes very close to the unscreened LO

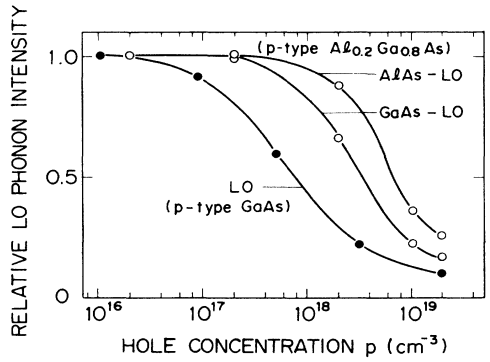


FIG. 9. Raman intensities of two LO-phonon branches of $p$-type $Al_{0.2}Ga_{0.8}As$ layers as a function of hole concentration. For reference, the intensity of the LO-phonon mode of $p$-type GaAs is also plotted. The experimental data are normalized by the Raman intensities for $p=1\times10^{16}$ cm$^{-3}$.

phonons have the high intensities because of the large phonon content, and therefore the LO-phonon modes including the unseparated coupled modes maintain the high intensity. The $L_+$ and $L_0$ modes in $p$-type $Al_{0.2}Ga_{0.8}As$ layers separate from the GaAs-like and AlAs-like LO phonons, respectively, at higher hole concentrations, compared to the peak separation of the high-frequency coupled mode $A$ in $p$-type GaAs layers, as shown in Figs. 1 and 6.

Self-energy effects, which cause the shift to lower energies and broadening of the TO-phonon Raman lines, have been reported for $p$-type GaAs (Ref. 8) as well as $n$- and $p$-type Si,[18] and $p$-type Ge (Ref. 8) with the Fermi level either above the conduction-band minima or below the top of the valence bands. The effects have been successfully explained by the interaction between electronic excitations and phonons through deformation-potential mechanism.[8,18] A long-wavelength optical vibration of the lattice is similar to an externally applied stress. The lattice vibrations, being displacements of sublattices with respect to each other, produce splittings of the energy bands similar to those produced by shear strains. Carriers in the energy bands redistribute until equilibrium is restored. When the redistribution time is comparable with the phonon frequency, as in the case of the optical phonons, self-energy effects are induced as the result of a dynamical coupling with the free carriers, that is, the interaction between the phonon scattering and one electron excitation from filled to empty valence states. For Zn-doped $p$-type (110) GaAs, the self-energy effects were observed for samples with hole concentrations larger than $4\times10^{19}$ cm$^{-3}$ by Olego and Cardona.[8] Further, they have explained the increased linewidth of the Raman mode peaking around 271 cm$^{-1}$ in the heavily Zn-doped (100) GaAs by the wave-vector-dependent self-energy effects of the forbidden TO phonons, and reproduced the linewidth by the calculation using the imaginary part of the self-energy of the phonons with $q=q_{\max}$, where $q_{\max}$ is the wave vector which gives the largest density of states of the free-particle excitation.[9] The largest shift and broadening of the TO phonons occur at $q=q_{\max}$, and $q_{\max}$ is larger than the wave vector of exciting laser for the sample with hole concentration less than $1\times10^{20}$ cm$^{-3}$. The larger wave vector of $q_{\max}$ is allowed by the wave-vector nonconservation. However, our experimental results support the conservation of the wave vector, as shown in Fig. 5. Therefore, the use of $q_{\max}$ in the calculation for the linewidth is invalid. The smaller $q$ leads the narrower TO-phonon linewidth which does not correspond to the large broadening of the mode $B$. Actually, we have found the small broadening of the TO-phonon line for a sample with $p=2\times10^{19}$ cm$^{-3}$. Figure 10 shows the TO-phonon spectra from the (110) cleaved surface of $p$-type GaAs layer with $p=2\times10^{19}$ cm$^{-3}$ grown on the semi-insulating GaAs substrate. The measurement was carried out by the same method as that for Fig. 5. Spectra from both the epitaxial layer and the substrate are shown in Fig. 10. The peak shift to the lower-frequency side with the increase in hole concentration is 0.8 cm$^{-1}$, and the linewidths are 4.8 and 4.4 cm$^{-1}$ for the epitaxial layer and the substrate, respectively. Thus, the contribution of the self-energy effects of the forbidden TO

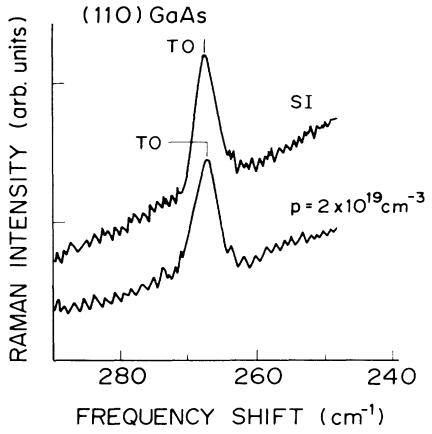


FIG. 10. Raman spectra from the (110) cleaved surfaces of both the epitaxial $p$-type GaAs layer with $p=2\times10^{19}$ cm$^{-3}$ and the semi-insulating GaAs substrate. The measurements were performed using a 514.5-nm focused Ar-ion laser beam.

phonons to the $B$ mode in $p$-type GaAs is negligible even though it occurs.

## V. CONCLUSIONS

The interaction of free holes with the optical phonons has been investigated in detail for the Raman spectra of Be-doped $p$-type GaAs and $p$-type $Al_{0.2}Ga_{0.8}As$ layers with various hole concentrations. Besides the LO phonons the spectra from the (100) surface of the heavily doped layers show the additional modes due to the hole-plasmon—LO-phonon coupling. On the other hand, the spectra from the (110) cleaved surface show the wave-vector conservation and the maintenance of the selection rule even in the layer with a high hole concentration of $2\times10^{19}$ cm$^{-3}$. The additional modes were assigned to the coupled modes by the hole-concentration and wave-vector dependence of their peak frequencies and dampings.

The coupled modes exhibit two branches of the high-frequency and the low-frequency modes in $p$-type GaAs, and three branches of the high-frequency, low-frequency, and intermediate-frequency modes in $p$-type $Al_{0.2}Ga_{0.8}As$. The behavior of the coupled hole-plasmon—LO-phonon modes is similar to that of the coupled electron-plasmon—LO-phonon modes. However, the coupled modes in the hole-plasmon—phonon system separate from the LO phonons at an order-of-magnitude-higher carrier concentration, and their dampings are much larger, as compared with those in the electron-plasmon—phonon system, because of the larger effective masses of free holes.

Self-energy effects of the TO phonons due to the coupling with the single-particle hole excitations have also been studied for the Raman spectra from the (110) cleaved surface by comparison with the spectrum of the semi-insulating substrate. The results of a heavily doped $p$-type GaAs layer with the hole concentration of $2\times10^{19}$ cm$^{-3}$ show the slight frequency shift and the small broadening of the TO-phonon line, and the negligible self-energy effects distinguish the broad low-frequency coupled mode near the TO phonons from the forbidden TO phonons in the spectrum from the (100) surface.

## ACKNOWLEDGMENTS

This research was supported by the Agency of Industrial Science and Technology, Ministry of International Trade and Industry, Japan.

*Present address: Opto-Electronics Research Laboratory, NEC Corporation, 4-1-1 Miyazaki, Miyamae-Ku, Kawasaki 213, Japan.

†Present address: LSI Research and Development Laboratory, Mitsubishi Electric Corporation, 4-1, Mizuhara, Itami 664, Japan.

[1]A. Mooradian and G. B. Wright, Phys. Rev. Lett. **16**, 999 (1966).

[2]A. Pinczuk, G. Abstreiter, R. Trommer, and M. Cardona, Solid State Commun. **21**, 959 (1977).

[3]G. Abstreiter, R. Trommer, M. Cardona, and A. Pinczuk, Solid State Commun. **30**, 703 (1979).

[4]G. Abstreiter, E. Bauser, A. Fisher, and K. Ploog, Appl. Phys. **16**, 345 (1978).

[5]T. Yuasa, S. Naritsuka, M. Mannoh, K. Shinozaki, K. Yamanaka, Y. Nomura, M. Mihara, and M. Ishii, Appl. Phys. Lett. **46**, 176 (1985).

[6]T. Yuasa, S. Naritsuka, M. Mannoh, K. Shinozaki, K. Yamanaka, Y. Nomura, M. Mihara, and M. Ishii, Phys. Rev. B **33**, 1222 (1986).

[7]F. Cerdeira, T. A. Fjeldly, and M. Cardona, Phys. Rev. B **8**, 4734 (1973).

[8]D. Olego and M. Cardona, Phys. Rev. B **23**, 6592 (1981).

[9]D. Olego and M. Cardona, Phys. Rev. B **24**, 7217 (1981).

[10]D. Olego and M. Cardona, Solid State Commun. **32**, 375 (1979).

[11]D. Olego and M. Cardona, Phys. Rev. B **22**, 886 (1980).

[12]M. Ilegems, J. Appl. Phys. **48**, 1278 (1977).

[13]G. Scott, G. Duggan, P. Dawson, and G. Weimann, J. Appl. Phys. **52**, 6888 (1981).

[14]W. T. Tsang, Appl. Phys. Lett. **34**, 473 (1979).

[15]R. K. Chang, J. M. Ralston, and D. E. Keating, in *Light-Scattering Spectra of Solids*, edited by G. B. Wright (Springer, New York, 1969), p. 369.

[16]B. A. Weinstein, Solid State Commun. **20**, 999 (1976).

[17]B. Varga, Phys. Rev. **137**, A1896 (1965).

[18]F. Cerdeira and M. Cardona, Phys. Rev. B **5**, 1440 (1972).

[19]O. K. Kim and W. G. Spitzer, Phys. Rev. B **20**, 3258 (1979).